THE JOURNAL OF BIOLOGICAL CHEMISTRY VOL. 291, NO. 51, pp. 26291–26303, December 16, 2016


# TP53-inducible Glycolysis and Apoptosis Regulator (TIGAR) Metabolically Reprograms Carcinoma and Stromal Cells in Breast Cancer*

Received for publication, May 31, 2016, and in revised form, October 17, 2016 Published, JBC Papers in Press, November 1, 2016, DOI 10.1074/jbc.M116.740209

**Ying-Hui Ko[‡], Marina Domingo-Vidal[‡], Megan Roche[‡], Zhao Lin[‡], Diana Whitaker-Menezes[‡], Erin Seifert[§], Claudia Capparelli[¶], Madalina Tuluc[§], Ruth C. Birbe[‖], Patrick Tassone[**], Joseph M. Curry[**], Àurea Navarro-Sabaté[‡‡], Anna Manzano[‡‡], Ramon Bartrons[‡‡], Jaime Caro[§§], and Ubaldo Martinez-Outschoorn[‡1]**

*From the [‡]Department of Medical Oncology, the [§]Department of Pathology, Anatomy, and Cell Biology, the [¶]Department of Cancer Biology, and the [**]Department of Otolaryngology, Sidney Kimmel Cancer Center, Thomas Jefferson University, Philadelphia, Pennsylvania 19107, [‖]Department of Pathology, Cooper University Hospital, Camden, New Jersey 08103, the [‡‡]Department of Physiological Sciences, University of Barcelona, Barcelona 08907, Spain, and the [§§]Department of Medicine, Cardeza Foundation for Hematological Research, Thomas Jefferson University, Philadelphia, Pennsylvania 19107*

**Edited by Jeffrey Pessin**

**A subgroup of breast cancers has several metabolic compartments. The mechanisms by which metabolic compartmentalization develop in tumors are poorly characterized. TP53 inducible glycolysis and apoptosis regulator (TIGAR) is a bisphosphatase that reduces glycolysis and is highly expressed in carcinoma cells in the majority of human breast cancers. Hence we set out to determine the effects of TIGAR expression on breast carcinoma and fibroblast glycolytic phenotype and tumor growth. The overexpression of this bisphosphatase in carcinoma cells induces expression of enzymes and transporters involved in the catabolism of lactate and glutamine. Carcinoma cells overexpressing TIGAR have higher oxygen consumption rates and ATP levels when exposed to glutamine, lactate, or the combination of glutamine and lactate. Coculture of TIGAR overexpressing carcinoma cells and fibroblasts compared with control cocultures induce more pronounced glycolytic differences between carcinoma and fibroblast cells. Carcinoma cells overexpressing TIGAR have reduced glucose uptake and lactate production. Conversely, fibroblasts in coculture with TIGAR overexpressing carcinoma cells induce HIF (hypoxia-inducible factor) activation with increased glucose uptake, increased 6-phosphofructo-2-kinase/fructose-2,6-bisphosphatase-3 (PFKFB3), and lactate dehydrogenase-A expression. We also studied the effect of this enzyme on tumor growth. TIGAR overexpression in carcinoma cells increases tumor growth *in vivo* with increased proliferation rates. However, a catalytically inactive variant of TIGAR did not induce tumor growth. Therefore, TIGAR expression in breast carcinoma cells promotes metabolic compartmentalization and tumor growth with a mitochondrial metabolic phenotype with lactate and glutamine catabolism. Targeting TIGAR warrants consideration as a potential therapy for breast cancer.**

Multiple metabolic compartments exist in human tumors including breast cancer (1). There is metabolic coupling with lactate transfer between highly glycolytic carcinoma cells and carcinoma cells with reduced glycolysis in models of vulvar and colon cancer (2). High stromal glycolysis with low cancer cell glycolysis have also been described in breast, ovarian, prostate, bladder, head and neck carcinomas, and sarcomas (3).

The interactions between carcinoma cells and fibroblasts in breast cancer play an important role in tumor progression. Fibroblasts have been shown to promote breast cancer tumor growth (4) and metastasis (5). Carcinoma cell invasiveness and resistance to chemotherapy in breast cancer are induced by fibroblasts (6). It is unknown how cancer cell metabolism in breast cancer modulates adjacent fibroblast metabolism.

TP53-induced glycolysis and apoptosis regulator (TIGAR)[2] is an inhibitor of glycolysis and is highly expressed in the majority of human breast-invasive ductal carcinomas (7, 8). TIGAR is the only known phosphatase glycolytic modulator regulated by TP53. It is unknown if TIGAR induces aggressive breast cancer. The human TIGAR gene is similar to the bisphosphatase domain of the glycolytic enzyme 6-phosphofructo-2-kinase/fructose-2,6-bisphosphatase (PFKFB) (7). TIGAR decreases glycolysis by functioning as a bisphosphatase that reduces levels

* This work was supported, in whole or in part, by National Institutes of Health Grants NCI K08-CA175193 and NCI 5 P30 CA 56036. This work was also supported by Instituto de Salud Carlos III-FIS (PI13/0096) and Fondo Europeo de Desarrollo Regional (FEDER). The authors declare that they have no conflicts of interest with the contents of this article. The content is solely the responsibility of the authors and does not necessarily represent the official views of the National Institutes of Health.

[1] To whom correspondence should be addressed: Dept. of Medical Oncology Sidney Kimmel Cancer Center, 233 S. 10th St. Suite 909. Philadelphia, PA 19107. Tel.: 215-955-9774; Fax: 215-955-2010; E-mail: ubaldo.martinez-outschoorn@jefferson.edu.

[2] The abbreviations used are: TIGAR, TP53-induced glycolysis and apoptosis regulator; PFKFB, 6-phosphofructo-2-kinase/fructose-2,6-bisphosphatase; Fru-2,6-$P_2$, fructose 2,6-bisphosphate; PFK-1, phosphofructokinase-1; OXPHOS, oxidative phosphorylation; MCT1 and -2, monocarboxylate transporter 1 and 2; LDH-B, lactate dehydrogenase B; GLS1, glutaminase 1; PGC1, peroxisome proliferator-activated receptor γ coactivator 1; NRF1, nuclear respiratory factor 1; OCR, oxygen consumption rate; TOMM20, transporter of the outer mitochondrial membrane member 20; 3PO, 3-(3-pyridinyl)-1-(4-pyridinyl)-2-propen-1-one; 2-NBDG, 2-(*N*-(7-nitrobenz-2-oxa-1,3-diazol-4-yl)amino)-2-deoxyglucose (fluorescent 2-deoxyglucose); HIF, hypoxia-inducible factor; RFP, red fluorescent protein; PI, propidium iodide.

of intracellular fructose-2,6-bisphosphate (Fru-2,6-$P_2$) and 2,3-bisphosphoglycerate (7, 9), which are regulators of glycolysis.

Phosphofructokinase-1 (PFK-1) is a key glycolytic enzyme that converts fructose 6-phosphate to fructose 1,6-bisphosphate. PFK-1 is allosterically activated by Fru-2,6-$P_2$ (10). Also, Fru-2,6-$P_2$ is an inhibitor of fructose-1,6-bisphosphatase, which opposes the activity of PFK-1 by converting fructose 1,6-bisphosphate to fructose 6-phosphate (10).

The synthesis and breakdown of Fru-2,6-$P_2$ depends on the bifunctional 6-phosphofructo-2-kinase/fructose-2,6-bisphosphatase isoenzymes, products of four genes (PFKFB1–4) that code for the different PFKFB isoenzymes and that have distinct cell expression patterns and display different kinase/bisphosphatase activity ratios and control by different protein kinases (10–12). In tumor cells, the concentration of Fru-2,6-$P_2$ is generally elevated due to overexpression and activation of PFKFB3, which has opposite effects of TIGAR (11–13). Conversely, TIGAR depletion increases glycolytic flux by increasing the activity of PFK-1 and the glycolytic flux by increasing Fru-2,6-$P_2$ levels (7, 14). It is unknown if TIGAR modulates catabolism of other substrates such as lactate and glutamine, which have been shown to be alternate catabolites to glucose for carcinoma cells (1). TIGAR expression has been shown to be inversely associated with glycolysis as TIGAR expression was inversely associated with 2-deoxyglucose uptake on PET scans in subjects with non-small cell lung cancer (15). TIGAR regulates hexokinase 2 (HK2) activity and increases mitochondrial membrane potential, but the effect of TIGAR on mitochondrial metabolism, oxygen consumption rates, and ATP generation is unknown (16). In sum, TIGAR reduces glycolysis, but its effects on the catabolism of other substrates and mitochondrial metabolism is poorly characterized.

TIGAR has been reported to mediate human cancer aggressiveness, although the mechanism is unclear, and its effect in breast cancer is unknown. In addition to reducing glycolysis, TIGAR reduces apoptosis (7). TIGAR is overexpressed in nasopharyngeal carcinoma, and genetic overexpression increases tumor growth with carcinoma cell growth, colony formation, migration, and invasion with NF$\kappa$B activation in carcinoma cells (17). Knockdown of this bisphosphatase induces apoptosis of HepG2 hepatocellular carcinoma cells (18). TIGAR down-regulation in HepG2 carcinoma cells reduces the size of hepatocellular carcinoma xenografts (19). TIGAR reduces apoptosis rates of non-small cell lung cancer H-1299 and osteosarcoma U2OS cells (7). TIGAR is also overexpressed in the majority of glioblastomas, protecting cells from starvation-induced cell death by up-regulating respiration and improving cellular redox homeostasis (20). Radiosensitization of glioma cells also occurs with TIGAR knockdown (14). However, another study has shown that TIGAR decreases cell viability in glioblastoma (21). TIGAR is required for proliferation of small intestine cells (22). TIGAR null mice have decreased tumorigenesis and increased survival in a model in which the tumor suppressor adenomatous polyposis coli (APC) is deleted in $LGR5^+$ intestinal stem cells (22). TIGAR is highly expressed in the majority of breast cancers and carcinoma cells in breast cancer frequently have low rates of glycolysis and apoptosis (7, 8, 24, and 25). However, no reports have described the effect of TIGAR on breast cancer tumor growth *in vivo*. Also, the role of TIGAR in the low rates of glycolysis and apoptosis with high proliferation observed in human breast cancer is unknown.

Breast tumors have high expression of mitochondrial biogenesis transcription factors and mitochondrial markers of oxidative phosphorylation (OXPHOS) (26) (27). Multiple metabolic compartments exist in human malignancies (28). Metabolic compartmentalization occurs in breast cancer with highly glycolytic stromal cells and cancer cells with high OXPHOS (28). There are no data on the metabolic effects of TIGAR expression in breast cancer and if it plays a role in metabolic compartmentalization or heterogeneity in tumors. We hypothesize that TIGAR expression in carcinoma cells induces aggressive disease with utilization of alternative catabolites to glucose and metabolic compartmentalization.

## Results

*TIGAR Induced Markers of Lactate and Glutamine Catabolism with Increased NADPH in Carcinoma Cells*—To investigate the effects of TIGAR on markers of lactate and glutamine utilization, we overexpressed TIGAR in breast carcinoma cells. TIGAR overexpression up-regulated moderately monocarboxylate transporter 2 (MCT2) protein and mRNA expression (Fig. 1, *A* and *B*). MCT2 is a lactate importer. TIGAR also up-regulates lactate dehydrogenase B (LDH-B), which is the enzyme that converts lactate into pyruvate for mitochondrial metabolism (Fig. 1*C*) and TIGAR up-regulates glutaminase 1 (GLS1) modestly, which is the rate-limiting enzyme in glutamine catabolism and converts glutamine to glutamate (Fig. 1*D*). Conversely, glutamate ammonia ligase (GLUL), which is the enzyme that mediates glutamine synthesis from glutamate and ammonia, was down-regulated with TIGAR overexpression (Fig. 1*E*). TIGAR markedly decreased the $NADP^+$/NADPH ratio (Fig. 1, *F* and *G*), which is consistent with increasing flux through the pentose phosphate pathway.

*TIGAR Induced OXPHOS and ATP Generation in the Presence of Lactate and Glutamine*—To investigate the effects of TIGAR on mitochondrial biogenesis, we studied the expression of peroxisome proliferator-activated receptor $\gamma$ coactivator 1 (PGC1) and nuclear respiratory factor 1 (NRF1). TIGAR overexpression induced these markers of mitochondrial biogenesis (Fig. 2*A*).

To investigate the effects of TIGAR and exposure to glutamine and lactate on OXPHOS, we studied oxygen consumption rates (OCR) in control and TIGAR-overexpressing carcinoma cells. Oxygen consumption rates were higher for TIGAR overexpressing carcinoma cells exposed to glutamine, lactate, or glutamine and lactate compared with carcinoma cells expressing the control vector ($p < 0.05$) (Fig. 2*B*). TIGAR overexpressing carcinoma cells exposed to glutamine have a 1.2-fold greater OCR than control carcinoma cells exposed to glutamine ($p < 0.05$) and 1.5-fold greater OCR when exposed to lactate or glutamine and lactate than the control carcinoma cells exposed to the same conditions ($p < 0.05$). OCRs were not increased by glutamine or lactate in the absence of TIGAR overexpression. TIGAR overexpressing carcinoma cells had lower OCR than control cells (0.8-fold) when cultured with glucose but without glutamine and lactate ($p < 0.05$).

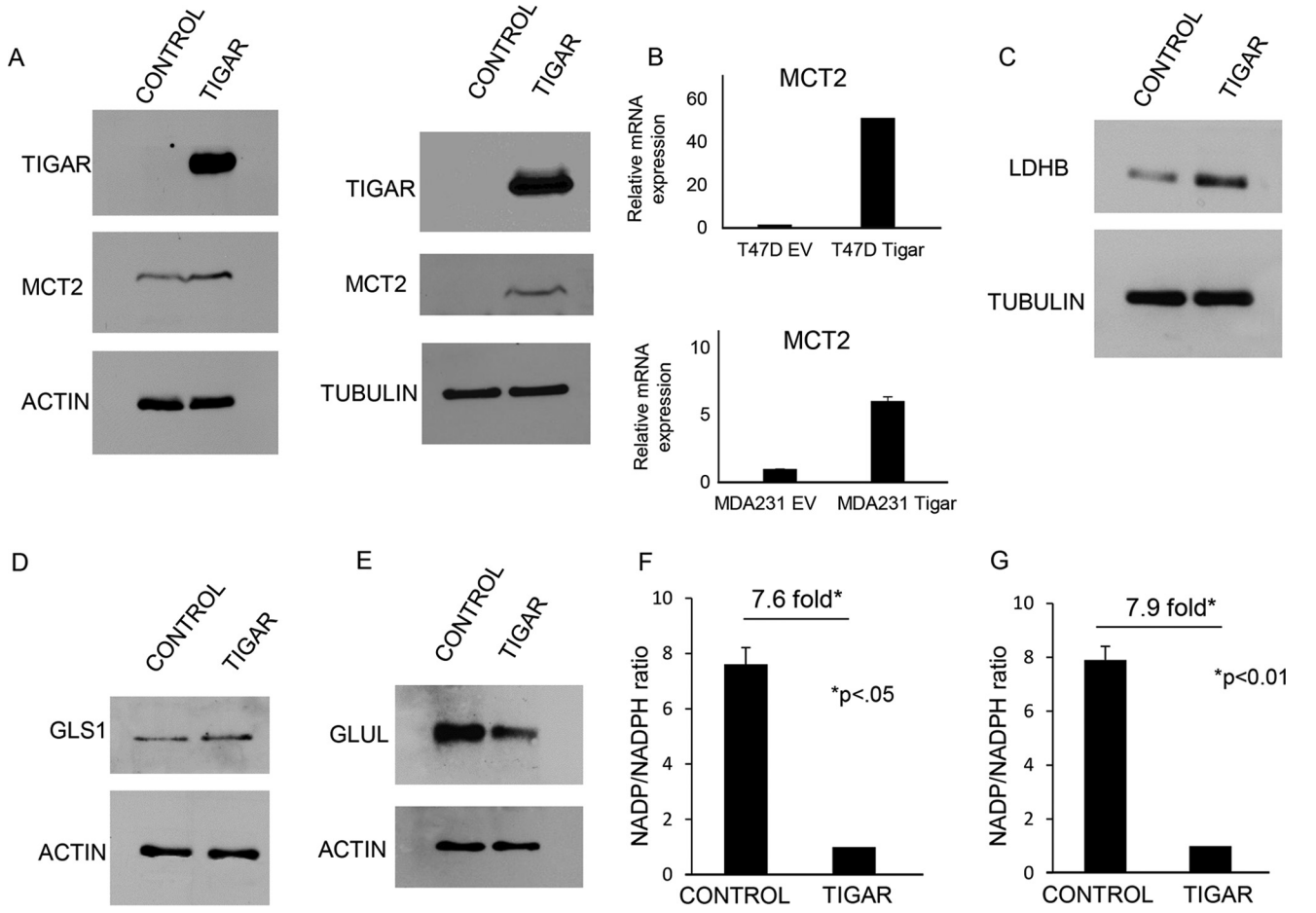


FIGURE 1. **Effect of TIGAR on markers of catabolism and NADPH in carcinoma cells.** T47D cells and MDA-MB-231 cells overexpressing TIGAR and control cells were cultured and lysed and subjected to immunoblot analysis for TIGAR and MCT2 (*A*), MCT2 mRNA expression as -fold change relative to control (*B*), LDHB protein expression (*C*), GLS1 protein expression (*D*), and GLUL (glutamate ammonia ligase) protein expression in T47D cells (*E*), $NADP^+$/NADPH ratio in T47D and MDA-MB-231 cells (*F* and *G*) .

Next, we studied the markers of OXPHOS metabolism MITONEET, and Transporter of the Outer Mitochondrial Membrane Member 20 (TOMM20). Both MITONEET and TOMM20 are up-regulated by TIGAR (Fig. 2*C*). TOMM20 overexpression in carcinoma cells also increased expression of TIGAR (Fig. 2*D*). Exposure of carcinoma cells to lactate, glutamine, or glutamine and lactate increased ATP generation (Fig. 2*E*).

We then exposed control and TIGAR-overexpressing carcinoma cells to 3-(3-pyridinyl)-1-(4-pyridinyl)-2-propen-1-one (3PO), which is a PFKFB3 inhibitor that reduces Fru-2,6-$P_2$ levels. Control cells exposed to 3PO do not have a significant change in ATP levels (Fig. 2*F*). However, TIGAR-overexpressing cells exposed to 3PO increased ATP levels (Fig. 2*F*).

*Fibroblasts Induced Aggressive T47D Cells with Increased TIGAR Expression, Reduced Expression of Glycolytic Markers, Increased Proliferation, and Decreased Apoptosis*—To investigate stromal-epithelial interactions, we used a coculture model system composed of 1) human fibroblasts immortalized with the telomerase catalytic domain (hTERT-BJ1 fibroblasts) and 2) T47D or MCF7 cells, which are well established breast cancer cell lines.

TIGAR and PFKFB3 are markers of glycolysis, although they have opposite effects. TIGAR mRNA expression was increased 1.5-fold in T47D cells in coculture ($p < 0.01$) (Fig. 3*A*) and 1.6-fold in MCF7 cells in coculture ($p < 0.05$), whereas PFKFB3 mRNA expression was reduced 1.9-fold in MCF7 cells in coculture ($p < 0.05$) (Fig. 3*B*). No statistically significant difference in PFKFB3 mRNA expression was noted in T47D cells in coculture (Fig. 3*A*).

Fibroblasts induced TIGAR expression in carcinoma cells (Fig. 3*C*), and TIGAR induced aggressive carcinoma cells with increased proliferation and reduced apoptosis. Carcinoma cells cocultured with fibroblasts had a 4.7-fold increase in DNA synthesis at the expense of $G_0$-$G_1$ and $G_2$-M ($p < 0.01$) (Fig. 3*D*). Carcinoma cells also had a 2-fold decreased apoptosis rate when in coculture with fibroblasts ($p < 0.05$) (Fig. 3*E*).

*TIGAR Reduced Glycolysis in Carcinoma Cells and Increases Glycolysis in Fibroblasts*—We studied 2-deoxyglucose uptake in T47D cells overexpressing TIGAR in coculture with fibroblasts by measuring fluorescence of 2-(*N*-(7-nitrobenz-2-oxa-1,3-diazol-4-yl)amino)-2-deoxyglucose (2-NBDG), which is a green fluorescent 2-deoxyglucose compound. 2-NBDG uptake correlates with glycolysis with higher uptake indicating increased glycolysis. T47D cells overexpressing TIGAR had a 1.3-fold reduced 2-NBDG uptake compared with control T47D cells in coculture ($p < 0.05$) (Fig. 4*A*). T47D cells overexpressing TIGAR in homotypic culture had no statistically significant

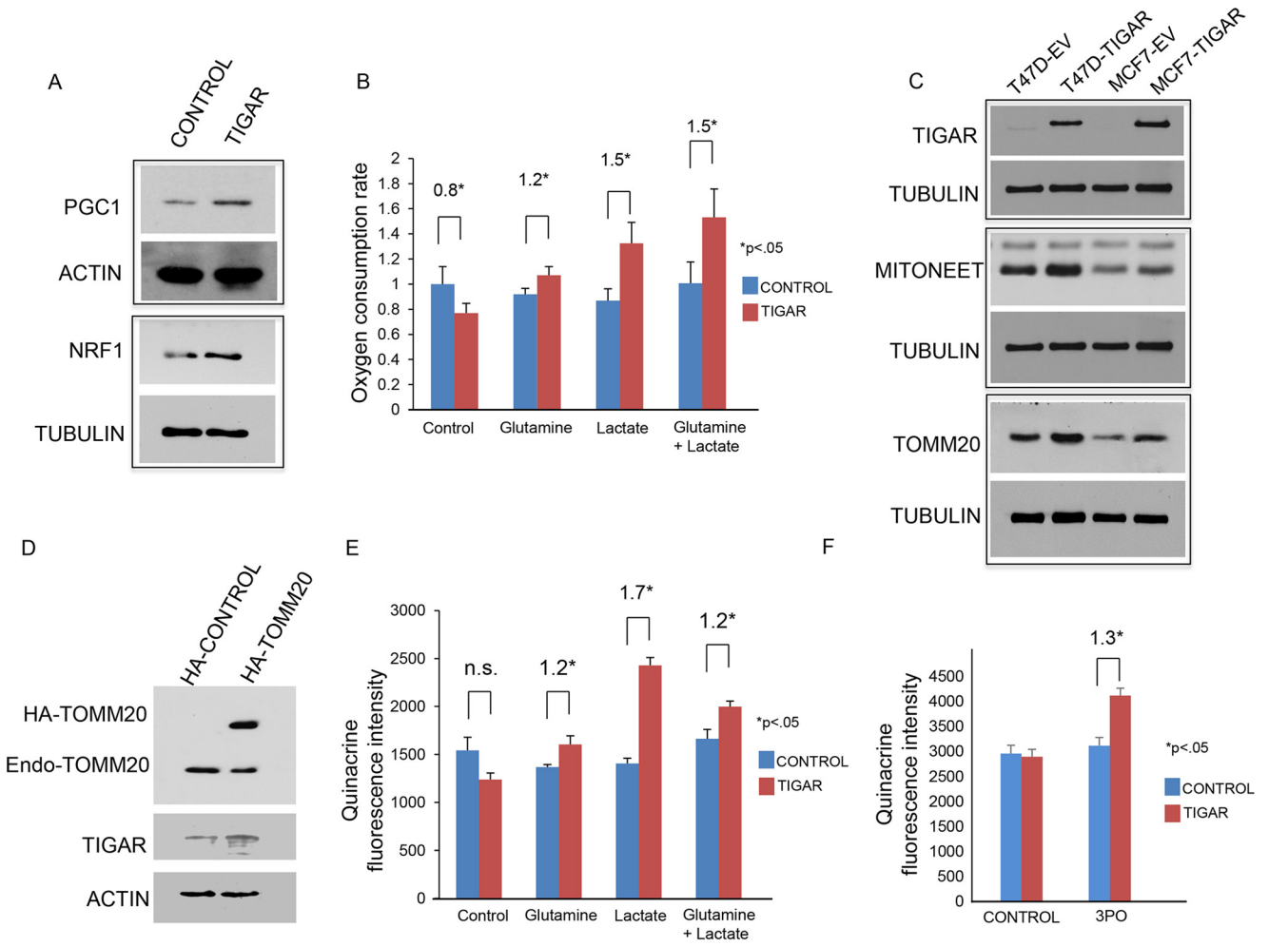


FIGURE 2. **Effect of TIGAR on mitochondria.** T47D cells overexpressing TIGAR and control cells were cultured and lysed and subjected to immunoblot analysis for PGC1 and NRF1 (*A*). *B*, oxygen consumption was measured in control T47D cells (*blue bar*) and with TIGAR overexpression (*red bar*); relative concentration is shown. Cells were cultured with control media, control with 2 mM glutamine, control with 10 mM lactate, or control with 2 mM glutamine and 10 mM lactate. *C*, T47D and MCF7 cells overexpressing TIGAR and control cells were cultured and lysed and subjected to immunoblot analysis for MITONEET and TOMM20. *D*, MCF7 cells overexpressing HA-TOMM20 were cultured and lysed and subjected to immunoblot analysis for TOMM20, TIGAR, and actin. *E*, ATP levels measured by quinacrine fluorescence intensity in TIGAR overexpressing and control MCF7 cells. Cell culture conditions as described above in *B*. *F*, ATP levels in TIGAR overexpressing and control MCF7 cells with or without 10 $\mu$M 3PO. *n.s.*, not significant.

difference in 2-NBDG uptake compared with control T47D cells (data not shown). T47D cells overexpressing TIGAR had a 1.9-fold reduced lactate production compared with control T47D cells ($p < 0.05$) (Fig. 4*B*). TOMM20 overexpression in carcinoma cells also reduced lactate production 1.9-fold ($p < 0.05$) (Fig. 4*C*). Lactate production is a measure of glycolysis with lower lactate levels indicating lower glycolysis. Hence the effect of TIGAR on glycolysis can be phenocopied by expression of TOMM20. Monocarboxylate transporter 1 (MCT1) is the main importer of lactate into cells and is inversely related to rates of glycolysis. TIGAR overexpression in carcinoma cells up-regulated MCT1 protein expression (Fig. 4*D*). Conversely TIGAR down-regulation in carcinoma cells using CRISPR-Cas9 reduced MCT1 expression (Fig. 4*E–F*).

*TIGAR in Carcinoma Cells Induced a Glycolytic Phenotype in Fibroblasts*—Next we studied the effect of TIGAR overexpression in T47D cells on fibroblast metabolism. Fibroblasts cocultured with T47D cells overexpressing TIGAR had a 1.2-fold increase in 2-NBDG uptake compared with fibroblasts in control cocultures ($p < 0.05$) (Fig. 5*A*). Glucose uptake in fibroblasts was measured by quantifying green fluorescence of the 2-deoxyglucose compound 2-NBDG. 2-Deoxyglucose and 2-NBDG uptake is an additional measure of glycolysis with lower uptake indicating reduced glycolysis. PFKFB3 and LDH-A expression increased in fibroblasts cocultured with TIGAR overexpressing carcinoma cells (Fig. 5, *B* and *C*). PFKFB3 and LDH-A are markers of glycolysis. LDH-B expression is reduced with coculture with TIGAR overexpressing carcinoma cells (Fig. 5*C*). LDH-B has opposite effects to LDH-A, converting lactate to pyruvate. We next assessed the effect of TIGAR on activation of hypoxia-inducible factor (HIF) in fibroblasts by using a HIF1A luciferase reporter as HIF1A is one of the main glycolytic transcription factors. NIH3T3 fibroblasts stably transfected with a HIF1A luciferase reporter were cultured with control T47D cells or TIGAR-overexpressing T47D cells. Activation of HIF1A is increased by 1.6-fold ($p < 0.05$) in fibroblasts cocultured with T47D cells overexpressing TIGAR cells in 0.5% $O_2$ hypoxia compared with control coculture conditions (Fig. 5*D*). Note that there was no significant change in HIF1A activation in normoxia between control coculture and

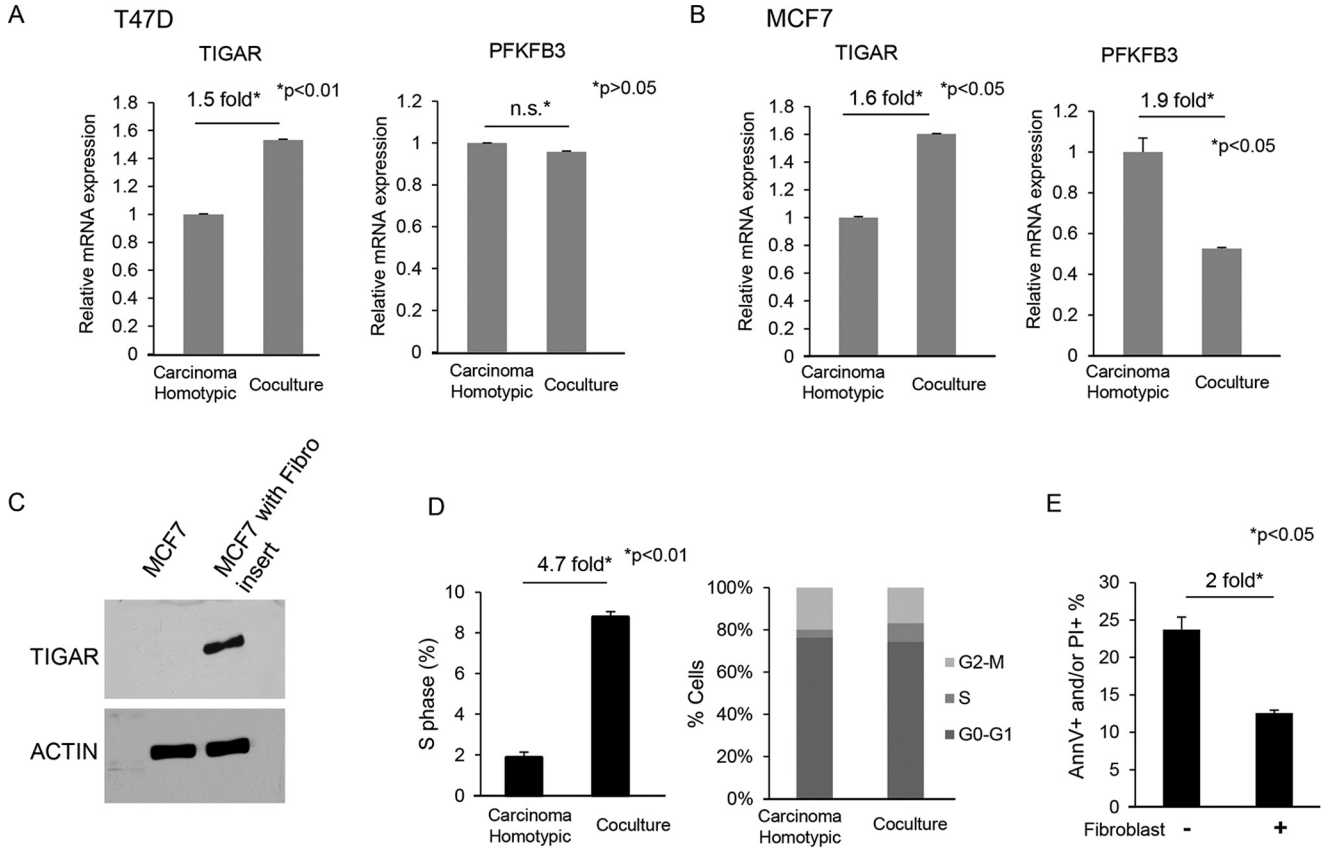


FIGURE 3. **Effect of coculture with fibroblasts on proliferation and apoptosis of carcinoma cells.** TIGAR and PFKFB3 mRNA in T47D (*A*) and MCF7 (*B*) cells in homotypic culture or coculture with fibroblasts. *n.s.*, not significant. *C*, MCF7 cells were cultured with fibroblasts using an insert and lysed and subjected to immunoblot analysis for TIGAR. *D*, DNA synthesis in carcinoma cells in homotypic culture or coculture with fibroblasts. T47D cells were cultured alone or in coculture with fibroblasts for 4 days. DNA synthesis was measured with EdU incorporation and the cell cycle was assessed in carcinoma cells in homotypic culture or coculture with fibroblasts. DNA synthesis was measured with EdU incorporation and ploidy assessment with propidium iodide. *E*, apoptosis in carcinoma cells in homotypic culture or coculture with fibroblasts. T47D cells were cultured alone or in coculture with fibroblasts for 4 days. Apoptosis was measured with annexin-V (*AnnV*) and propidium iodide (PI) staining. The percentage of apoptotic or dead T47D cells (annexin-V-positive and/or PI-positive) is shown.

coculture with T47D cells overexpressing TIGAR. Fibroblasts exposed to carcinoma cells have reduced TIGAR expression, but overexpression of TIGAR in fibroblasts led to 1.2-fold reduced glucose uptake compared with control fibroblasts (Fig. 5*E*). In sum, TIGAR overexpression in carcinoma cells induced a glycolytic phenotype in fibroblasts.

*TIGAR Induced Tamoxifen Resistance but Higher Sensitivity to Mitochondrial Modulators*—T47D cells were cultured alone or with fibroblasts and exposed to tamoxifen. TIGAR overexpression in carcinoma cells exposed to tamoxifen induced apoptosis resistance with a 1.2-fold reduction in homotypic culture and a 1.4-fold reduction in coculture with fibroblasts ($p < 0.05$) (Fig. 6*A*). In contrast, TIGAR-overexpressing carcinoma cells were more sensitive to apoptosis by mitochondrial modulators. Metformin, which is an OXPHOS complex I inhibitor, doxycycline, which inhibits mitochondrial translation, and ABT-199, which inhibits BCL2 as a single agent or in combination induced higher rates of apoptosis in TIGAR-overexpressing T47D cells than controls (Fig. 6, *B–E*). Exposure to lactate in MCF7 cells led to increased TIGAR and BCL2 expression with reduced MCT4 expression (Fig. 6*F*). Exposure to tamoxifen in MCF7 cells decreased expression of TIGAR, BCL-XL, BCL2, MITONEET, and labile subunits of OXPHOS (Fig. 6, *G–H*). Overexpression of MITONEET in MCF7 cells, which is a marker of OXPHOS, reduced apoptosis rates in coculture with tamoxifen 1.3-fold ($p < 0.05$) (Fig. 6*I*).

*TIGAR Overexpression Increased Xenograft Size*—MDA-MB-231, T47D, and MCF7 cells overexpressing TIGAR and control cells were injected into the mammary gland of nude female mice. MDA-MB-231 cells overexpressing TIGAR had reduced Fru-2,6-$P_2$ levels compared with controls (Fig. 7*A*). MDA-MB-231 tumors with TIGAR-overexpressing carcinoma cells had 2.5-fold greater volume ($p < 0.05$) and 2.4 greater weight ($p < 0.05$) than control tumors (Fig. 7*B*).

TIGAR-overexpressing T47D tumors had higher TOMM20 expression than controls (Fig. 7*C*). TIGAR-overexpressing T47D cells had reduced Fru-2,6-$P_2$ levels compared with controls (Fig. 7*D*). T47D tumors with TIGAR-overexpressing carcinoma cells had 3.5-fold greater volume ($p < 0.05$) and 3.8-fold greater weight ($p < 0.05$) than control tumors (Fig. 7*E*). Mitotic figures were increased 1.5-fold ($p < 0.05$) in TIGAR overexpressing tumors compared with controls (Fig. 7*F*).

TIGAR-overexpressing MCF7 cells had reduced Fru-2,6-$P_2$ levels compared with controls (Fig. 7*G*). MCF7 tumors with TIGAR-overexpressing carcinoma cells had 7.8-fold greater volume ($p < 0.05$) and 5-fold greater weight ($p < 0.15$) than

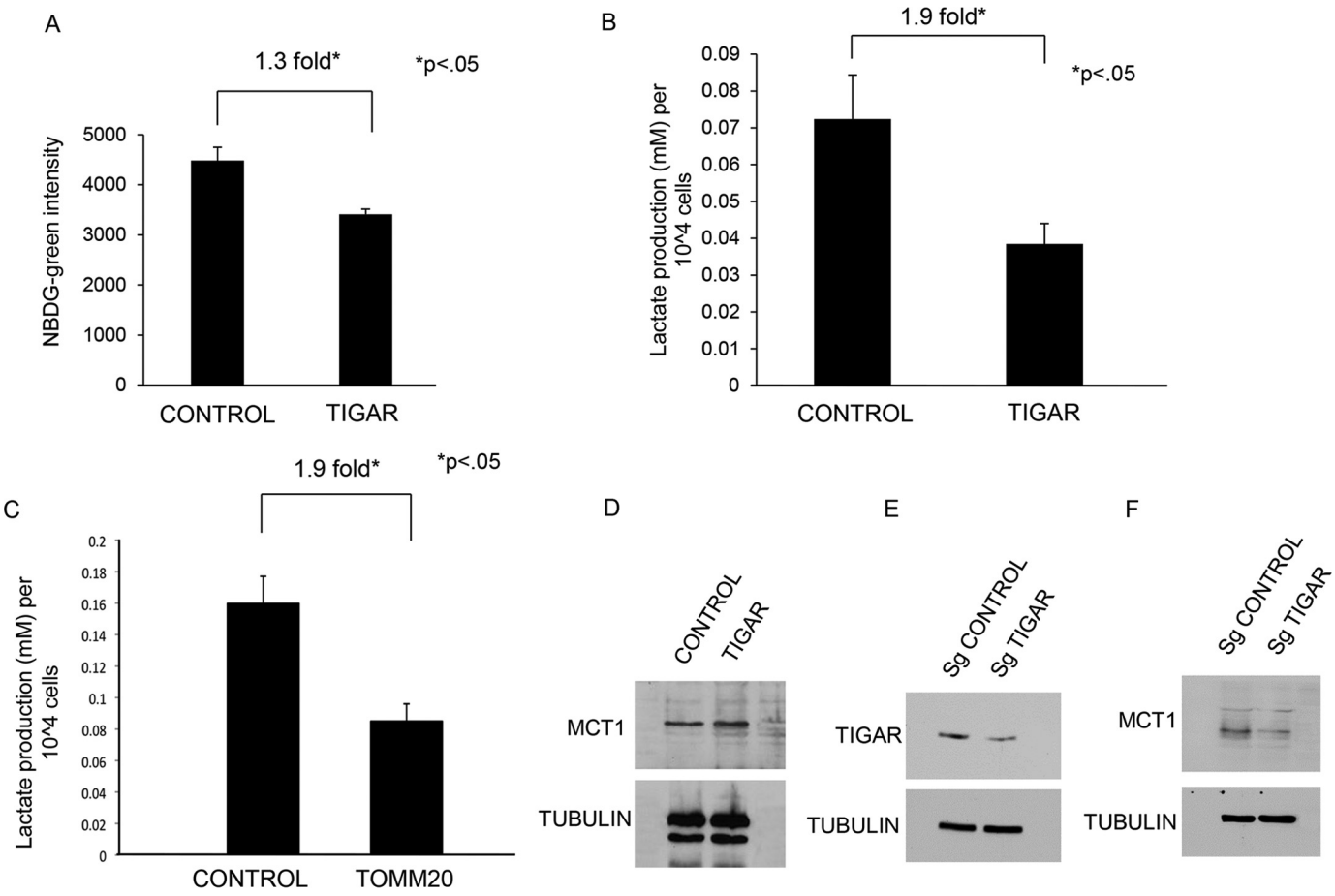


FIGURE 4. **Effect of TIGAR on glycolysis and MCT1 in carcinoma cells.** *A*, glucose uptake in TIGAR overexpressing carcinoma cells in coculture. RFP-tagged fibroblasts were cocultured with T47D cells either overexpressing TIGAR or control T47D cells. NBDG uptake in T47D cells was measured by flow cytometry. *B*, lactate production in TIGAR overexpressing carcinoma cells. Lactate production in T47D cells was measured and normalized to cell number. *C*, lactate production in HA-TOMM20-overexpressing carcinoma cells. Lactate production in MCF7 cells was measured and normalized to cell number. *D*, MCF7-overexpressing TIGAR and control T47D cells were cultured and lysed and subjected to immunoblot analysis for MCT1. MCF7 with TIGAR down-regulation and control cells using CRISPR-Cas9 were cultured and lysed and subjected to immunoblot for TIGAR (*E*) and MCT1 (*F*).

control tumors (Fig. 7*H*). Mitotic figures were increased 5.6-fold ($p < 0.05$) in TIGAR-overexpressing tumors compared with controls (Fig. 7*I*).

TIGAR-overexpressing T47D tumors had higher expression of BCL2 than controls. Cells staining strongly positive for BCL2 by digital pathology quantification (3+ intensity) were increased 3-fold in TIGAR-overexpressing tumors ($p < 0.05$) (Fig. 8*A*).

MDA-MB-231 cells overexpressing TIGAR with three mutations (H11A/E102A/H198A) that render it catalytically inactive as a Fru-2,6-$P_2$ bisphosphatase (TIGAR triple mutant) were generated. The triple mutant TIGAR as expected did not reduce Fru-2,6-$P_2$ levels and did not increase tumor growth compared with control carcinoma cells (Fig. 8*B*). Hence, a catalytically active TIGAR is required to promote tumor growth.

## Discussion

The current study delineates the role of TIGAR in OXPHOS and glycolytic metabolic reprogramming in breast cancer. This bisphosphatase enzyme, which reduces Fru-2,6-$P_2$ levels, inhibits glycolysis and increases pentose phosphate pathway flux with increased $NADP^+$ to NADPH production. We have discovered that TIGAR promotes the growth of breast-invasive ductal carcinoma *in vivo* and with utilization of lactate and glutamine as substrates, mitochondrial OXPHOS metabolism, and ATP generation in cancer cells (Figs. 2 and 8*C*). Increased ATP levels in TIGAR-overexpressing cells upon exposure to 3PO suggests that TIGAR provides metabolic flexibility with changes in Fru-2,6-$P_2$ levels. We also demonstrate that TIGAR expression in carcinoma cells induces reciprocal metabolic changes in fibroblasts (Figs. 5 and 8*D*).

Our finding that TIGAR promotes growth of breast-invasive ductal carcinoma is relevant to human disease because high TIGAR expression is found in the majority of patients with these tumors (8). A catalytically active TIGAR is required to promote tumor growth. However, other activities of TIGAR may also influence the biological properties of tumor cells.

Drugs targeting TIGAR's bisphosphatase activity may be beneficial in the management of breast-invasive ductal carcinoma. Inhibitors of complex I of OXPHOS such as metformin, of mitochondrial translation such as doxycycline, and BCL2 such as ABT-199 might have higher affinity in TIGAR-overexpressing tumors and will need to be studied further. Conversely, TIGAR overexpression induces resistance to the antiestrogen drug tamoxifen *in vitro*, and future studies will need to determine whether TIGAR expression predicts responsiveness to

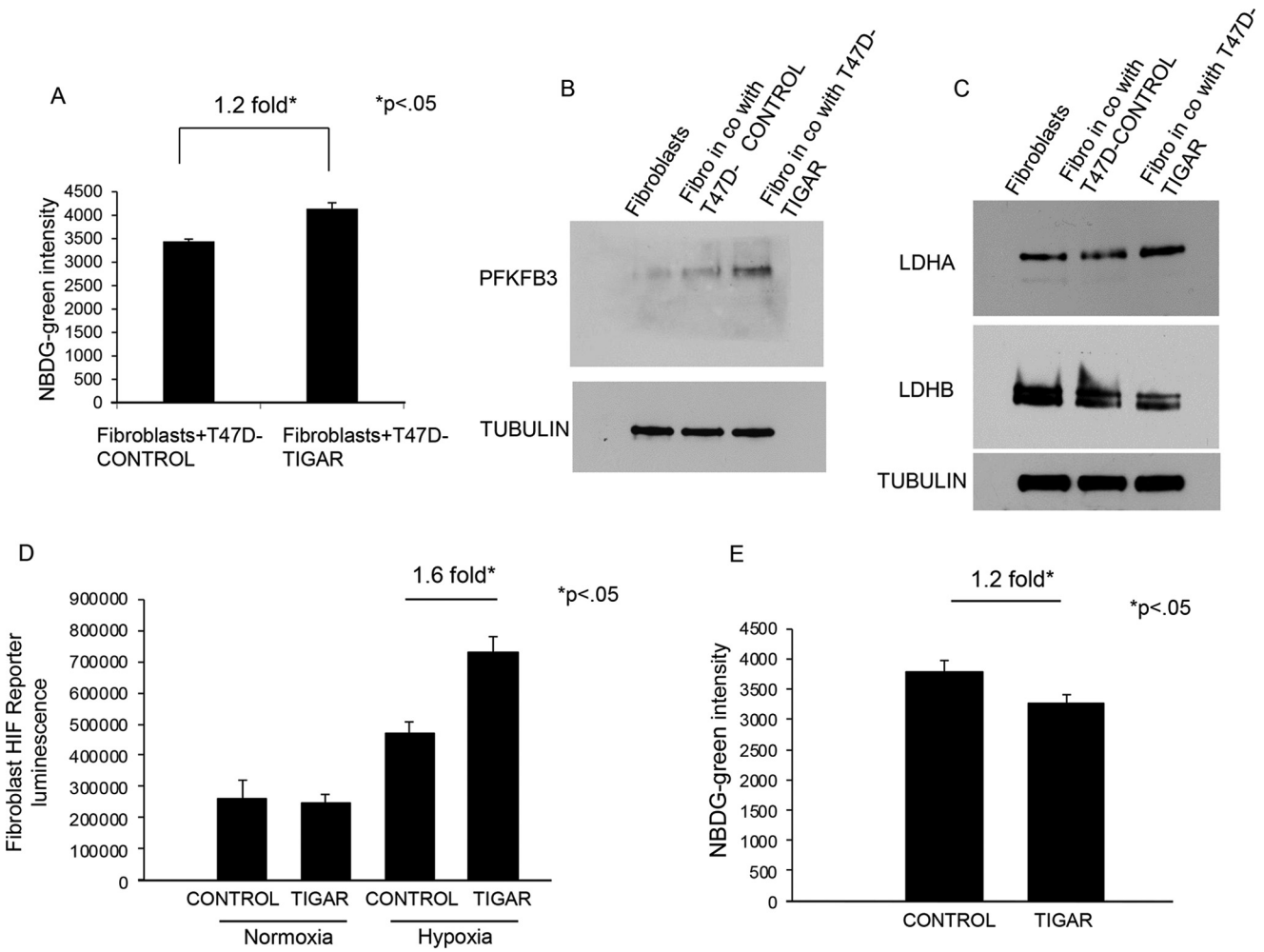


FIGURE 5. **Effect of carcinoma TIGAR expression on fibroblast glycolysis.** *A*, glucose uptake in fibroblasts cocultured with TIGAR-overexpressing carcinoma cells. RFP-tagged fibroblasts were cocultured with T47D cells either overexpressing TIGAR or control T47D cells. NBDG uptake was measured by flow cytometry. *B* and *C*, fibroblasts with a GFP tag were cocultured with T47D cells either overexpressing TIGAR or control vectors. Fibroblasts were then lysed and subjected to immunoblot analysis for PFKFB3 (*B*) and LDHA and LDHB (*C*). HIF1A luciferase reporter in fibroblasts in coculture with carcinoma cells overexpressing TIGAR or control vector. Coculture was performed in normoxia (21% $O_2$) or hypoxia (0.5% $O_2$) (*D*). *E*, glucose uptake in fibroblasts overexpressing TIGAR. Fluorescent 2-deoxyglucose uptake was measured by flow cytometry using 2-NBDG.

tamoxifen in women with hormone receptor-positive breast cancer. Resveratrol has been shown to reduce TIGAR expression, and research into drugs targeting TIGAR is being conducted (29).

TIGAR is regulated by TP53, TP73, SP1, and AKT and indirectly by MYC, c-Met, and miR-144 (7, 30–35). It is important to note that although TP53 up-regulates TIGAR expression experimentally, its expression in human breast cancer is inversely correlated to the expression of TP53 (8). Future work will need to determine the main drivers of TIGAR expression in breast cancer.

TIGAR is an enzyme that reduces glycolysis (7). TIGAR overexpression in carcinoma cells reduced glycolysis, as expected in the current study, and increased OXPHOS in these cells. Aggressive cancer cells with low glycolysis and high pentose phosphate activity have been described (36). High OXPHOS is also associated with aggressive cancer (26, 37). The current study demonstrates that TIGAR induces reciprocal metabolic changes in adjacent fibroblasts with enhanced glycolysis compared with the metabolic effects in carcinoma cells. The increased fibroblast glycolysis in the current study occurred in the context of increased PFKFB3 and LDH-A expression with HIF1A activation. HIF1A is one of the main glycolytic transcription factors, and it regulates the expression of PFKFB3 and LDH-A. TIGAR in carcinoma cells also led to reduced LDH-B and reduced TIGAR expression in fibroblasts which increase glycolysis. It has been shown that glycolytic fibroblasts increase breast cancer aggressiveness and tumor growth (38) (39). In sum, the current study demonstrates that TIGAR induces aggressive breast cancer with metabolic reprogramming of the tumor microenvironment with low glycolysis in carcinoma cells and opposite changes in stromal cells. Future studies will need to determine the contribution of the metabolic state of carcinoma cells and stromal cells to breast cancer tumor growth.

The current study demonstrates that TIGAR expression in carcinoma cells reduces TIGAR expression in wild-type TP53 fibroblasts. TIGAR is regulated by TP53 (7). Additional factors that regulate TIGAR expression in carcinoma cells are likely to modulate TIGAR expression in fibroblasts. For example,

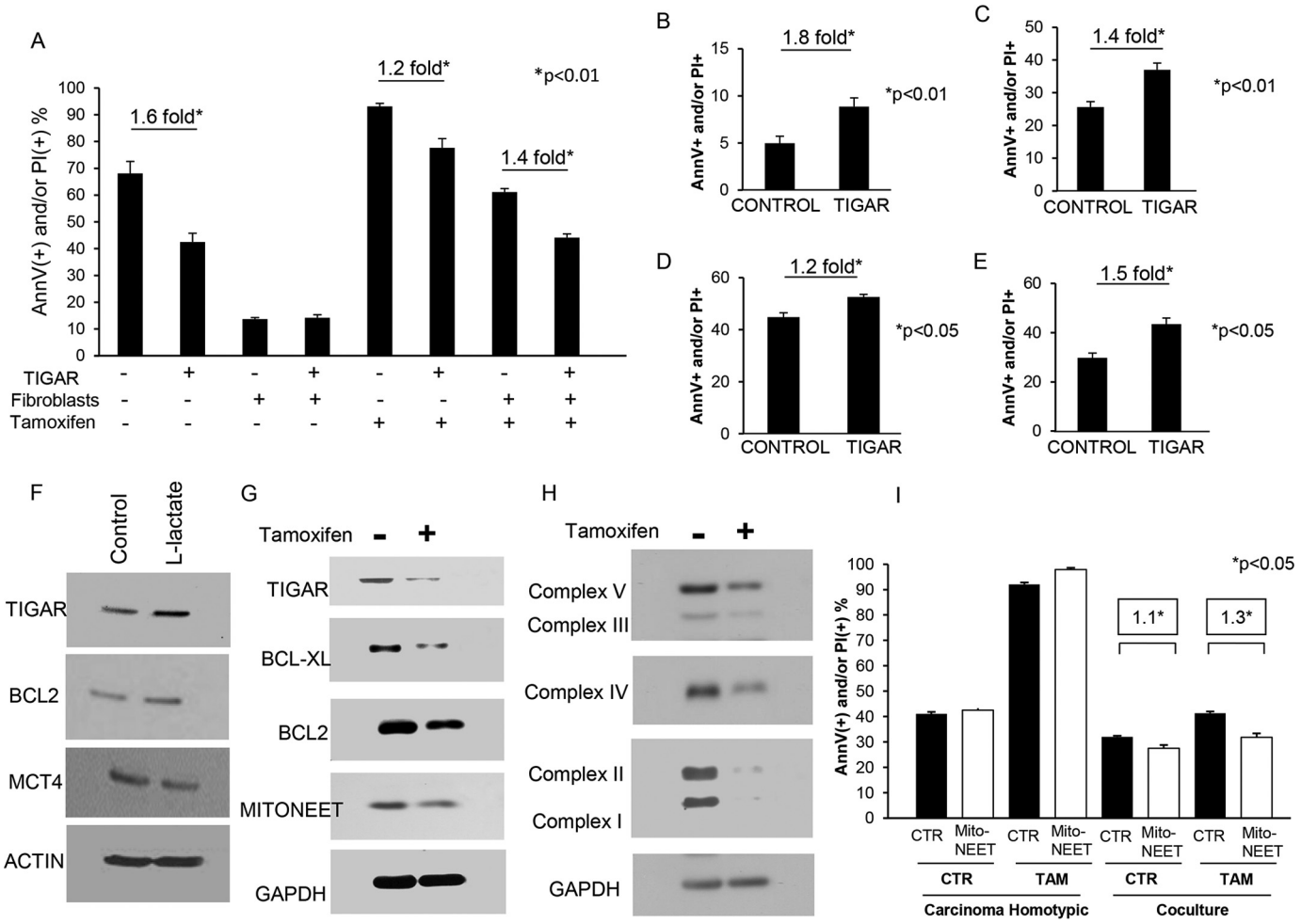


FIGURE 6. **Effect of TIGAR on chemotherapy-induced apoptosis.** T47D cells overexpressing TIGAR or control T47D cells were cultured alone or in coculture with fibroblasts for 2 days. Cells were incubated for 48 h with and without 10 $\mu$M tamoxifen (*A*), 200 $\mu$M metformin (*B*), 15 $\mu$M doxycycline (*C*), 5 $\mu$M ABT-199 (*D*) and with metformin, doxycycline, and ABT-199 (*E*). Apoptosis was measured with annexin-V and PI staining. The percentage of apoptotic or dead T47D cells (annexin-V-positive and/or PI-positive) is shown. *F*, expression of metabolic and mitochondrial markers in carcinoma cells exposed to lactate. MCF7 cells were cultured with DMEM medium with 10% FBS overnight. Then cells were incubated with and without 10 mM lactate for 48 h. Cells were then lysed and subjected to immunoblot analysis for TIGAR, MCT4, and BCL2. Actin was used as loading control. *G* and *H*, expression of markers of mitochondrial function in carcinoma cells exposed to tamoxifen. MCF7 cells were cultured with DMEM medium with 10% FBS overnight. Then cells were incubated with and without 10 $\mu$M tamoxifen for 48 h. Cells were then lysed and subjected to immunoblot analysis for TIGAR, BCL-XL, BCL2, MITONEET (*G*), and OXPHOS labile subunits (*H*). GAPDH was used as loading control. *I*, MCF7 cells overexpressing MITONEET or control MCF7 cells were cultured alone or in coculture with GFP-tagged fibroblasts for 2 days. Then, cells were incubated with and without 10 $\mu$M tamoxifen for 48 h. Apoptosis rate was measured as in *A*.

TIGAR expression is also regulated by the transcription factors MYC and SP1 (31, 33, 40, 41). TIGAR is also regulated by NF$\kappa$B and PHD1 (42). Hence, MYC and SP1 may regulate TIGAR expression in breast cancer-associated fibroblasts. Also, TP53 mutations in breast cancer-associated fibroblasts may alter TIGAR expression as TP53 mutations and deletions alter TIGAR expression in carcinoma cells (7, 22, 40). Carcinoma cells favor the selection of fibroblasts lacking wild-type TP53 (43). TP53 mutations have been demonstrated in breast cancer-associated fibroblasts (44). In addition, fibroblasts from patients with Li-Fraumeni syndrome have an abnormal TP53, as the syndrome is due to germ line abnormalities in TP53. In conclusion, high glycolysis in breast cancer-associated fibroblasts is induced by high TIGAR expression in carcinoma cells. The role of additional modulators of glycolysis such as MYC, SP1, and abnormal TP53 in breast cancer-associated fibroblasts needs to be studied.

This study reveals that TIGAR can induce tumor metabolic compartmentalization with highly glycolytic fibroblasts and carcinoma cells with reduced glycolysis and high OXPHOS. The effects of TIGAR on glycolysis, OXPHOS, and ATP are similar to the changes in marker expression by Western blot in this study. HIF1A activation in fibroblasts was studied to determine the potential mechanisms by which TIGAR overexpression in carcinoma cells induces metabolic asymmetry with increased fibroblast glycolysis. Glycolysis is induced upon HIF1A activation (10) (45, 46). The current study demonstrates that HIF1A is activated in fibroblasts when TIGAR is overexpressed in carcinoma cells. It has been previously shown that HIF1A activation in breast cancer-associated fibroblasts promotes tumor growth (47). The contribution of fibroblast HIF1A activation to increased glycolysis, increased PFKFB3 expression, and tumor growth will need to be determined in future studies.

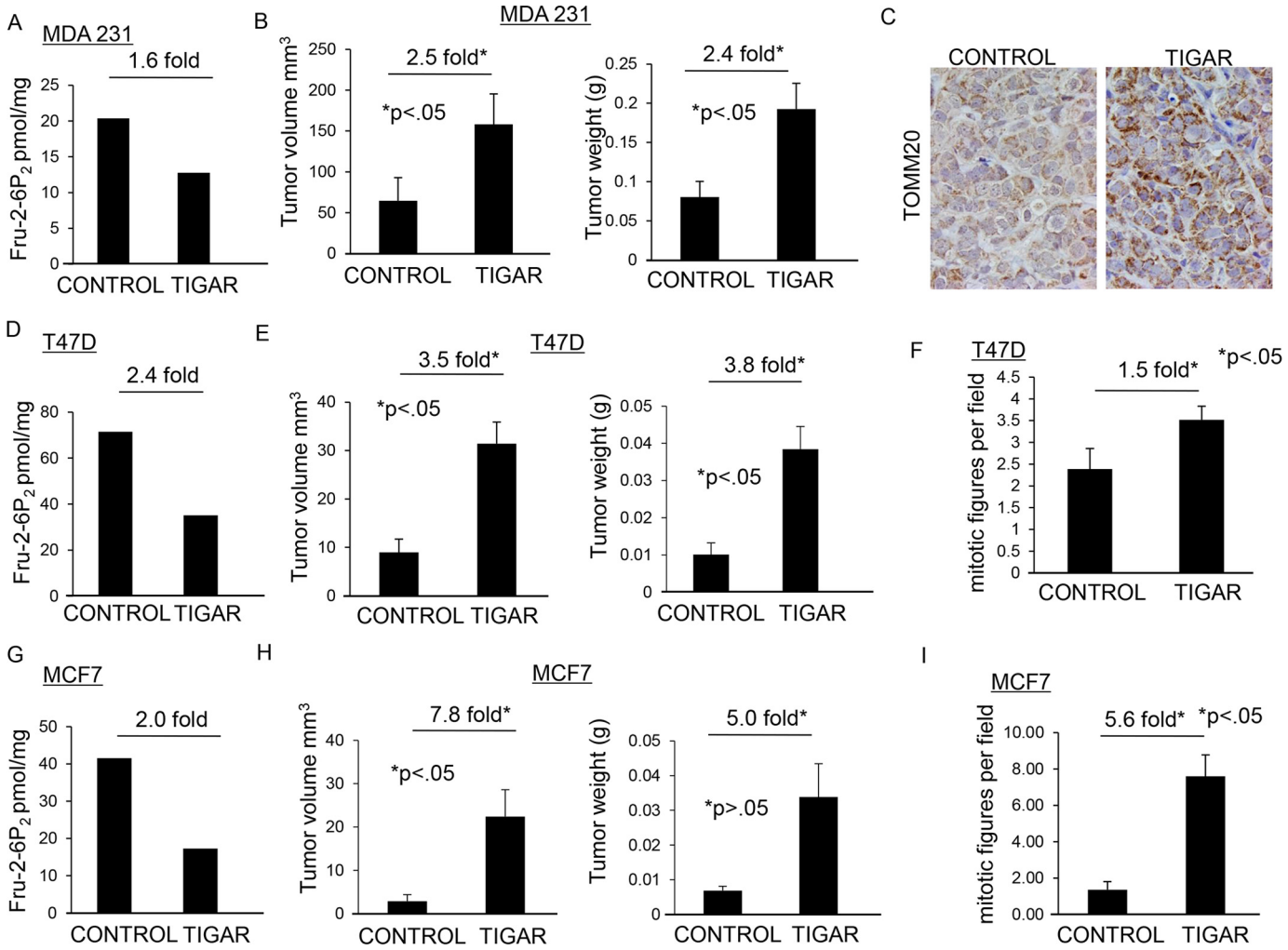


FIGURE 7. **Effect of TIGAR in carcinoma cells on orthotopic tumor growth and proliferation.** *A*, Fru-2,6-$P_2$ levels. MDA-MB-231 cells overexpressing TIGAR or empty vector control were cultured, and Fru-2,6-$P_2$ levels were measured. *B*, tumor growth. MDA-MB-231 cells overexpressing TIGAR (MDA-MB-231-TIGAR) or empty vector control were injected into the mammary fat pad of nude mice. Tumor volume and weight were measured after resection at 4 weeks post-injection. *C*, TOMM20 expression. T47D tumors overexpressing TIGAR or empty vector control tumor sections were stained by immunohistochemistry for TOMM20. Original magnification is 40×. *D*, Fru-2,6-$P_2$ levels in T47D-TIGAR or control cells. *E*, tumor growth. T47D-TIGAR or control cells were injected into the mammary fat pad of nude mice. Tumor volume and weight were measured after resection at 4 weeks post-injection. *F*, proliferation rates. Mitotic figures in T47D tumors were quantified per high power field. *G*, Fru-2,6-$P_2$ levels. MCF7 cells overexpressing TIGAR or empty vector control were cultured, and Fru-2,6-$P_2$ levels were measured. *H*, tumor growth. MCF7-TIGAR or control cells were injected into the mammary fat pad of nude mice. Tumor volume and weight were measured after resection at 4 weeks post-injection. *I*, proliferation rates. Mitotic figures in MCF7 tumors were quantified per high power field.

In sum, the current study provides mechanistic information on how TIGAR regulates fibroblast-carcinoma cell metabolic interactions in breast cancer. It has long been recognized that fibroblasts in proximity to cancer cells are pro-tumorigenic (4, 48). Most studies have focused on how fibroblast-secreted factors lead to a fibroblast-activated state that promotes tumor growth (4, 49). We set out to determine how the metabolic state of carcinoma cells modulates cancer aggressiveness and the metabolic phenotype of fibroblasts. TIGAR expression in breast carcinoma cells drives a mitochondrial OXPHOS phenotype in these carcinoma cells with a glycolytic phenotype in fibroblasts with increased tumor growth *in vivo*. Further work will need to determine the precise contribution of each of these factors to cancer aggressiveness.

## Experimental Procedures

*Materials*—Materials were obtained as follows: NADP/NADPH quantification colorimetric kit (BioVision K347-100), Click-iT® EdU Flow Cytometry Assay kit (Life Technologies C10418), lactate assay kit (EnzyChrom™ ECLC-100), quinacrine dihydrochloride (Sigma, Q3251), 3PO (EMD 525330), doxycycline (Sigma, D9891), metformin (Sigma D150959), ABT-199 (Selleck Chemicals, S8048), TIGAR and PFKFB3 primers (Hs00608644 and Hs00190079, Applied Biosystems), and MCT2 primers (forward sequence, GGTGATAGCAGGAGGCTTATT, and reverse sequence, GTTGCAGGTTGAAGGCTAAAC) (GeneCopoeia). Antibodies were obtained as follows: GLS1 (ab60709, Abcam), MCT1 (SC-365501, Santa Cruz Biotechnology), MCT2 (SC-50322, Santa Cruz Biotechnology), MCT4 (SC-50329, Santa Cruz Biotechnology), LDH-A (ab101562, Abcam), LDH-B (AV48210, Sigma), PGC1 (ab72230, Abcam), NRF1 (ab55744, Abcam), TIGAR (SC-166291, Santa Cruz Biotechnology), TOMM20 (SC-17764, Santa Cruz Biotechnology), MITONEET (16006–1-AP, Proteintech), B-actin (A5441, Sigma), tubulin (T4026, Sigma), GAPDH (CS 2118, Cell Signaling), OXPHOS labile subunit

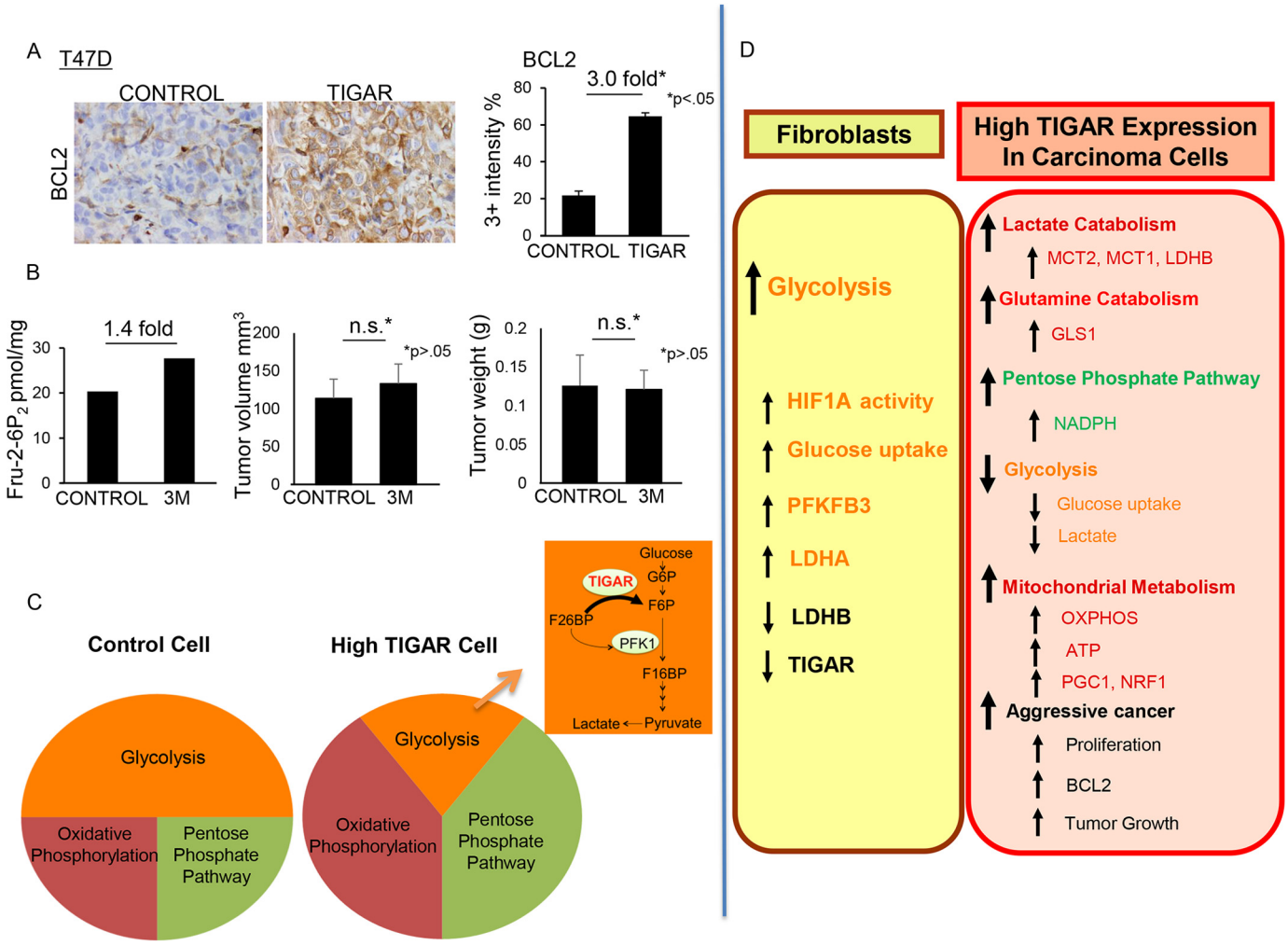


FIGURE 8. **TIGAR and BCL2, tumor growth with catalytically inactive TIGAR, and models of TIGAR effects on carcinoma and fibroblast cells.** *A*, BCL2 expression. Tumor sections were stained by immunohistochemistry for BCL2. Original magnification is 40×. The percentage of cells with the strongest BCL2 protein expression was quantified by Aperio digital pathology (3+ intensity percentage). *B*, Fru-2,6-$P_2$ levels and tumor growth. MDA-MB-231 cells overexpressing triple mutant TIGAR with H11A/E102A/H198A mutations (MDA-MB-231-TIGAR-3M) or empty vector control were cultured, and Fru-2,6-$P_2$ levels were measured. MDA-MB-231 cells overexpressing triple mutant TIGAR (MDA-MB-231-TIGAR-3M) or empty vector control were injected into the mammary fat pad of nude mice. Tumor volume and weight were measured after resection at 4 weeks post-injection. No statistically significant change in volume or weight was noted between triple mutant TIGAR and control cells. *C*, a model is shown of how TIGAR expression in carcinoma cells reduces glycolysis, increases the pentose phosphate pathway activity, and increases mitochondrial oxidative phosphorylation. *D*, high TIGAR expression in carcinoma cells alters their metabolic state and induces cancer aggressiveness. Conversely, fibroblasts in proximity to carcinoma cells have reciprocal metabolic changes.

mixture (MS601, Abcam), BCL2 (ab7973 and ab182858, Abcam for immune blot and immunohistochemistry, respectively), and BCL-XL (CS 2764, Cell Signaling).

*Cell Culture*—The human breast carcinoma cell lines (T47D, MCF7, and MDA-MB-231) were purchased from ATCC. Human skin fibroblasts immortalized with human telomerase reverse transcriptase catalytic domain (hTERT-BJ1) were purchased from Clontech, and clones were generated with green fluorescent protein (GFP) or red fluorescent protein (RFP) overexpression. Cells were passaged for fewer than 6 months after resuscitation. Cells were cultured in media containing 5 mM glucose and 1 mM pyruvate, 10% fetal bovine serum, 100 units/ml penicillin, and 100 units/ml streptomycin in a 37 °C, 5% $CO_2$ incubator. RPMI 1640 was the base medium for T47D cells and DMEM for MCF7 and MDA-MB-231 as recommended by ATCC. To study the effect of lactate and glutamine, control conditions were compared with those with 2 mM glutamine or 10 mM lactate or 2 mM glutamine plus 10 mM lactate.

*Co-culture System*—Fibroblasts and carcinoma cells were cocultured as previously described (50). Briefly, cells were seeded at a 3:1 fibroblast to carcinoma cell ratio, and the total number of cells per well was $1 \times 10^5$. As controls, cultures of fibroblasts and carcinoma cells alone were plated in parallel with the same number of cells of a given type as in coculture ($7.5 \times 10^4$ fibroblasts and $2.5 \times 10^4$ carcinoma cells).

*Messenger RNA Quantification*—Total RNA was extracted using the RNeasy Mini Kit(Qiagen). Complementary DNA (cDNA) was randomly primed from 2.0 $\mu$g of total RNA using the SuperScript III First-Strand Synthesis System for RT-PCR (Invitrogen). Real-time PCR was performed in triplicate with a 1:3 dilution of cDNA using the Power SYBR Green PCR system. Relative expression levels were determined using the comparative $\Delta\Delta$Ct method. All mRNA quantification data were normalized to $\beta$-actin.

*TIGAR, TOMM20, and MITONEET Overexpression and TIGAR Down-regulation*—TIGAR (EX-W1314-Lv105), TIGAR triple mutant (H11A/E102A/H198A, CS-W1314-Lv105),

MITONEET (EX-V0831-Lv105), empty vector control (EX-NEG-Lv105), HA-TOMM20 (EX-G0283-Lv120), HA control (EX-NEG-LV120) vectors and Cas9 nuclease lentiviral expression clone (CP-LvC9NU-01), Sg RNA lentiviral expression targeting C12orf5 (HCP215394-LvSG03-3-10), and Sg RNA lentiviral control (CCPCTR01-LvSG03) were purchased from GeneCopoeia, and lentiviruses were prepared according to the manufacturer's protocol. Virus-containing media were centrifuged, filtered (0.45 $\mu$M polyethersulfone (PES) low protein filter), and stored in 1-ml aliquots at −80 °C. Carcinoma cells (120,000 cells/well) were plated in 12-well dishes in growth media. After 24 h the media was removed and replaced with 250 $\mu$l of media with 5% FBS, 150 $\mu$l of virus-containing media, and 5 $\mu$g/ml Polybrene. 24 h post-infection the media-containing virus was removed and replaced with growth media. The cells were selected with puromycin (2 $\mu$g/ml) for 3 days after infection.

*Measurement of NADP/NADPH Ratio*—Plated cells were washed and centrifuged at 2000 rpm for 5 min. Extraction buffer was admixed with two freeze and thaw cycles. NADP cycling enzyme was added as well as the NADPH developer, and measurement was at $A_{450\ nm}$.

*OCR Assessment*—A Seahorse Bioscience XF96 Extracellular Flux Analyzer in a 24-well format was used. T47D cells were preseeded in the XF24 24-well plate with 100 $\mu$l of RPMI 1640 media with 10% fetal bovine serum, 100 units/ml penicillin, 100 units/ml streptomycin, 1 mM pyruvate and additional 2 mM glutamine and/or 10 mM lactate in a 37 °C, 5% $CO_2$ incubator for 2 h. After 2 h, an additional 200 $\mu$l of growth medium was added for a total volume of 300 $\mu$l per well. On the second day, cells were incubated in non-buffered RPMI 1640 media for 2 h. Measurements were obtained under basal conditions. OCR was normalized to total protein content. Statistical significance was examined using Student's $t$ test. Values of $p < 0.05$ were considered significant.

*ATP Assay*—Intracellular ATP levels were measured using the ATP-sensitive fluorochrome quinacrine. Briefly, cells were incubated with 20 $\mu$M quinacrine dihydrochloride at 37 °C for 1 h, and green fluorescence intensity was measured by flow cytometry as previously described (51).

*Apoptosis Assessment*—Apoptosis in culture was quantified by flow cytometry using PI and annexin-V-APC as previously described (50).

*Measurement of Glucose Uptake*—2-NBDG, which is green fluorescent 2-deoxyglucose, was utilized as previously described (47).

*Proliferation Assessment*—For DNA content and proliferation analyses, cells were incubated with EdU (Click-iT® EdU Flow Cytometry Assay kits) for 1 h. Then cells were stained with propidium iodide and anti-EdU-APC antibody. Cells were then analyzed by flow cytometry for nascent DNA synthesis (EdU incorporation) and ploidy assessment (PI). Proliferating cells in the xenograft tumors were identified on the basis of mitotic figures. Cells were counted in all fields within the central area of each tumor excluding regions with stromal elements using a 20× objective lens and an ocular grid (0.25 $mm^2$ per field). The total numbers of mitotic figures per unit area was calculated, and the data were represented graphically.

*Two Cell Populations Sorting by Flow Cytometry*—Fibroblasts with an RFP tag were cultured alone or in coculture with carcinoma cells for 4 days. Two cell populations were separated by flow cytometry through sorting with RFP-positive and RFP-negative cells. The presence of RFP in fibroblasts and lack of color in carcinoma cells allows us to separate these two cell populations in the flow cytometry cell sorter. After cell sorting, cells were then lysed and subjected to immunoblot analysis.

*Measurement of Lactate Production*—$10 \times 10^4$ of cells were plated in each well of a 12-well plate with cell culture medium, and on the 2nd day the medium was changed to RPMI 1640 with 2% FBS. After 24 h, cell media were collected and lactate production was analyzed as described (47).

*Luciferase Activity*—NIH3T3 fibroblasts stably transfected with a HIF1A luciferase reporter (RC0017, Panomics) were seeded in co-culture with carcinoma control or carcinoma TIGAR carcinoma cells. As controls, fibroblasts were plated in mono-culture using the same cell numbers as in the corresponding co-cultures. Luciferase activity was measured as previously described (52).

*Fru-2,6-$P_2$* Determination—Fru-2,6-$P_2$ was determined as previously described (53), and protein concentration was determined by the Bradford assay (Bio-Rad).

*Immunohistochemistry*—Sections were deparaffinized, rehydrated through graded ethanol, and washed in PBS. Antigen retrieval was performed in 0.01 M citrate buffer, pH 6.0, for 10 min using a pressure cooker followed by blocking for endogenous peroxidase in 3% $H_2O_2$ for 15 min. An avidin-biotin kit (Biocare Medical) was used to block endogenous biotin. For BCL2 rabbit antibody (ab 182858, Abcam), sections were blocked with 10% goat serum and incubated with antibody for 1 h at room temperature. After washing in PBS, the sections were incubated with biotinylated goat anti-rabbit IgG (Vector Laboratories) for 30 min and then avidin-horseradish peroxidase complex (Vectastain Elite ABC kit, Vector) for 30 min. Antibody reactivity was detected using liquid DAB substrate chromagen (Dako). For TOMM20 the Vector M.O.M. Basic kit was used followed by ABC and DAB detection. Quantitative analysis of immunohistochemistry was performed employing Aperio software as previously described (54). Increasing intensity using Aperio was quantified as 0, 1+, 2+ and 3+.

*Animal Studies*—To evaluate the *in vivo* tumor-promoting effects of TIGAR, mammary gland injections were performed on female athymic NCr nude mice (NCRNU; Taconic Farms; at 6 weeks of age). All animals were maintained in a pathogen-free environment/barrier facility at the Kimmel Cancer Center at Thomas Jefferson University. Experiments were performed according to National Institutes of Health guidelines. The Institutional Animal Care and Use Committee (IACUC) approved all animal protocols. MDA-MB-231, MCF7, and T47D cells were injected into the mammary fat pads of nude mice. Cancer cells (1 million cells) and (0.3 million) hTERT-BJ1 fibroblasts were resuspended in 100 $\mu$l of sterile PBS just before injection into the mammary fat pad. Oophorectomy and estrogen supplementation with 17$\beta$-estradiol pellet placement (0.72 mg/pellet) were performed before injection of the estrogen receptor-positive cell lines MCF7 and T47D as previously described (23). After 4 weeks post-injection, tumors were

excised to determine their weight and size. Volumes were calculated using the formula $V = (X^2Y)/2$, where $V$ is the tumor volume, $x$ is the length of the short axis, and $y$ is the length of the long axis using electronic calipers. Statistical significance was examined using the Mann-Whitney $U$ test. Values of $p < 0.05$ were considered significant.

*Author Contributions*—Y.-H. K., Z. L., J. M. C., R. B., J. C., and U. M.-O. were involved in the study design and concept. A. N.-S., A. M., and R. B. provided the reagents. Y.-H. K., M. D.-V., M. R., Z. L., D. W.-M., C. C., A. N.-S., A. M., and P. T. were involved in data acquisition. Y.-H. K., M. D.-V., M. R., Z. L., D. W.-M., E. S., C. C., J. M. C., R. C. B., M. T., A. N.-S., A. M., R. B., J. C., and U. M.-O. were involved in data analysis and interpretation. Y. H. K. and U. M.-O. drafted the manuscript. Y.-H. K., J. M. C., R. B., J. C., and U. M.-O. edited the manuscript.

*Acknowledgments—We thank Jose Martinez and Michael Mastrangelo for the thoughtful discussions about this project. We also thank Steven Katz for support.*

## References


1. DeNicola, G. M., and Cantley, L. C. (2015) Cancer's fuel choice: new flavors for a picky eater. *Mol. Cell* **60,** 514–523
2. Sonveaux, P., Végran, F., Schroeder, T., Wergin, M. C., Verrax, J., Rabbani, Z. N., De Saedeleer, C. J., Kennedy, K. M., Diepart, C., Jordan, B. F., Kelley, M. J., Gallez, B., Wahl, M. L., Feron, O., and Dewhirst, M. W. (2008) Targeting lactate-fueled respiration selectively kills hypoxic tumor cells in mice. *J. Clin. Invest.* **118,** 3930–3942
3. Martinez-Outschoorn, U. E., Sotgia, F., and Lisanti, M. P. (2015) Caveolae and signalling in cancer. *Nat. Rev. Cancer* **15,** 225–237
4. Orimo, A., Gupta, P. B., Sgroi, D. C., Arenzana-Seisdedos, F., Delaunay, T., Naeem, R., Carey, V. J., Richardson, A. L., and Weinberg, R. A. (2005) Stromal fibroblasts present in invasive human breast carcinomas promote tumor growth and angiogenesis through elevated SDF-1/CXCL12 secretion. *Cell* **121,** 335–348
5. Karnoub, A. E., Dash, A. B., Vo, A. P., Sullivan, A., Brooks, M. W., Bell, G. W., Richardson, A. L., Polyak, K., Tubo, R., and Weinberg, R. A. (2007) Mesenchymal stem cells within tumour stroma promote breast cancer metastasis. *Nature* **449,** 557–563
6. Shekhar, M. P., Santner, S., Carolin, K. A., and Tait, L. (2007) Direct involvement of breast tumor fibroblasts in the modulation of tamoxifen sensitivity. *Am. J. Pathol* **170,** 1546–1560
7. Bensaad, K., Tsuruta, A., Selak, M. A., Vidal, M. N., Nakano, K., Bartrons, R., Gottlieb, E., and Vousden, K. H. (2006) TIGAR, a p53-inducible regulator of glycolysis and apoptosis. *Cell* **126,** 107–120
8. Won, K. Y., Lim, S. J., Kim, G. Y., Kim, Y. W., Han, S. A., Song, J. Y., and Lee, D. K. (2012) Regulatory role of p53 in cancer metabolism via SCO2 and TIGAR in human breast cancer. *Hum. Pathol.* **43,** 221–228
9. Gerin, I., Noël, G., Bolsée, J., Haumont, O., Van Schaftingen, E., and Bommer, G. T. (2014) Identification of TP53-induced glycolysis and apoptosis regulator (TIGAR) as the phosphoglycolate-independent 2,3-bisphosphoglycerate phosphatase. *Biochem. J.* **458,** 439–448
10. Okar, D. A., Manzano, A., Navarro-Sabatè, A., Riera, L., Bartrons, R., and Lange, A. J. (2001) PFK-2/FBPase-2: maker and breaker of the essential biofactor fructose-2,6-bisphosphate. *Trends Biochem. Sci.* **26,** 30–35
11. Bartrons, R., and Caro, J. (2007) Hypoxia, glucose metabolism and the Warburg's effect. *J. Bioenerg. Biomembr.* **39,** 223–229
12. Novellasdemunt, L., Bultot, L., Manzano, A., Ventura, F., Rosa, J. L., Vertommen, D., Rider, M. H., Navarro-Sabate, À., and Bartrons, R. (2013) PFKFB3 activation in cancer cells by the p38/MK2 pathway in response to stress stimuli. *Biochem. J.* **452,** 531–543
13. Atsumi, T., Chesney, J., Metz, C., Leng, L., Donnelly, S., Makita, Z., Mitchell, R., and Bucala, R. (2002) High expression of inducible 6-phosphofructo-2-kinase/fructose-2,6-bisphosphatase (iPFK-2; PFKFB3) in human cancers. *Cancer Res.* **62,** 5881–5887
14. Peña-Rico, M. A., Calvo-Vidal, M. N., Villalonga-Planells, R., Martínez-Soler, F., Giménez-Bonafé, P., Navarro-Sabaté, À., Tortosa, A., Bartrons, R., and Manzano, A. (2011) TP53 induced glycolysis and apoptosis regulator (TIGAR) knockdown results in radiosensitization of glioma cells. *Radiother. Oncol.* **101,** 132–139
15. Zhou, X., Xie, W., Li, Q., Zhang, Y., Zhang, J., Zhao, X., Liu, J., and Huang, G. (2013) TIGAR is correlated with maximal standardized uptake value on FDG-PET and survival in non-small cell lung cancer. *PLoS ONE* **8,** e80576
16. Cheung, E. C., Ludwig, R. L., and Vousden, K. H. (2012) Mitochondrial localization of TIGAR under hypoxia stimulates HK2 and lowers ROS and cell death. *Proc. Natl. Acad. Sci. U.S.A.* **109,** 20491–20496
17. Zhao, M., Fan, J., Liu, Y., Yu, Y., Xu, J., Wen, Q., Zhang, J., Fu, S., Wang, B., Xiang, L., Feng, J., Wu, J., and Yang, L. (2016) Oncogenic role of the TP53-induced glycolysis and apoptosis regulator in nasopharyngeal carcinoma through NF-κB pathway modulation. *Int. J. Oncol.* **48,** 756–764
18. Ye, L., Zhao, X., Lu, J., Qian, G., Zheng, J. C., and Ge, S. (2013) Knockdown of TIGAR by RNA interference induces apoptosis and autophagy in HepG2 hepatocellular carcinoma cells. *Biochem. Biophys. Res. Commun.* **437,** 300–306
19. Xie, J. M., Li, B., Yu, H. P., Gao, Q. G., Li, W., Wu, H. R., and Qin, Z. H. (2014) TIGAR has a dual role in cancer cell survival through regulating apoptosis and autophagy. *Cancer Res.* **74,** 5127–5138
20. Wanka, C., Steinbach, J. P., and Rieger, J. (2012) Tp53-induced glycolysis and apoptosis regulator (TIGAR) protects glioma cells from starvation-induced cell death by up-regulating respiration and improving cellular redox homeostasis. *J. Biol. Chem.* **287,** 33436–33446
21. Sinha, S., Ghildiyal, R., Mehta, V. S., and Sen, E. (2013) ATM-NFκB axis-driven TIGAR regulates sensitivity of glioma cells to radiomimetics in the presence of TNFα. *Cell Death Dis.* **4,** e615
22. Cheung, E. C., Athineos, D., Lee, P., Ridgway, R. A., Lambie, W., Nixon, C., Strathdee, D., Blyth, K., Sansom, O. J., and Vousden, K. H. (2013) TIGAR is required for efficient intestinal regeneration and tumorigenesis. *Dev. Cell* **25,** 463–477
23. Osborne, C. K., Hobbs, K., and Clark, G. M. (1985) Effect of estrogens and antiestrogens on growth of human breast cancer cells in athymic nude mice. *Cancer Res.* **45,** 584–590
24. Bensaad, K., Cheung, E. C., and Vousden, K. H. (2009) Modulation of intracellular ROS levels by TIGAR controls autophagy. *EMBO J.* **28,** 3015–3026
25. Li, L., Ishdorj, G., and Gibson, S. B. (2012) Reactive oxygen species regulation of autophagy in cancer: implications for cancer treatment. *Free Radic Biol. Med.* **53,** 1399–1410
26. Wallace, D. C. (2012) Mitochondria and cancer. *Nat. Rev. Cancer* **12,** 685–698
27. Sotgia, F., Whitaker-Menezes, D., Martinez-Outschoorn, U. E., Salem, A. F., Tsirigos, A., Lamb, R., Sneddon, S., Hulit, J., Howell, A., and Lisanti, M. P. (2012) Mitochondria "fuel" breast cancer metabolism: fifteen markers of mitochondrial biogenesis label epithelial cancer cells, but are excluded from adjacent stromal cells. *Cell Cycle* **11,** 4390–4401
28. Martinez-Outschoorn, U. E., Lisanti, M. P., and Sotgia, F. (2014) Catabolic cancer-associated fibroblasts transfer energy and biomass to anabolic cancer cells, fueling tumor growth. *Semin. Cancer Biol.* **25,** 47–60
29. Kumar, B., Iqbal, M. A., Singh, R. K., and Bamezai, R. N. (2015) Resveratrol inhibits TIGAR to promote ROS induced apoptosis and autophagy. *Biochimie* **118,** 26–35
30. Lee, P., Hock, A. K., Vousden, K. H., and Cheung, E. C. (2015) p53- and p73-independent activation of TIGAR expression in vivo. *Cell Death Dis.* **6,** e1842
31. Zou, S., Gu, Z., Ni, P., Liu, X., Wang, J., and Fan, Q. (2012) SP1 plays a pivotal role for basal activity of TIGAR promoter in liver cancer cell lines. *Mol. Cell Biochem* **359,** 17–23
32. Simon-Molas, H., Calvo-Vidal, M. N., Castaño, E., Rodríguez-García, A., Navarro-Sabaté, À., Bartrons, R., and Manzano, A. (2016) Akt mediates TIGAR induction in HeLa cells following PFKFB3 inhibition. *FEBS Lett.* **590,** 2915–2926

33. Cheung, E. C., Lee, P., Ceteci, F., Nixon, C., Blyth, K., Sansom, O. J., and Vousden, K. H. (2016) Opposing effects of TIGAR- and RAC1-derived ROS on Wnt-driven proliferation in the mouse intestine. *Genes Dev.* **30,** 52–63
34. Lui, V. W., Wong, E. Y., Ho, K., Ng, P. K., Lau, C. P., Tsui, S. K., Tsang, C. M., Tsao, S. W., Cheng, S. H., Ng, M. H., Ng, Y. K., Lam, E. K., Hong, B., Lo, K. W., Mok, T. S., Chan, A. T., and Mills, G. B. (2011) Inhibition of c-Met downregulates TIGAR expression and reduces NADPH production leading to cell death. *Oncogene* **30,** 1127–1134
35. Chen, S., Li, P., Li, J., Wang, Y., Du, Y., Chen, X., Zang, W., Wang, H., Chu, H., Zhao, G., and Zhang, G. (2015) MiR-144 inhibits proliferation and induces apoptosis and autophagy in lung cancer cells by targeting TIGAR. *Cell. Physiol. Biochem.* **35,** 997–1007
36. Pusapati, R. V., Daemen, A., Wilson, C., Sandoval, W., Gao, M., Haley, B., Baudy, A. R., Hatzivassiliou, G., Evangelista, M., and Settleman, J. (2016) mTORC1-dependent metabolic reprogramming underlies escape from glycolysis addiction in cancer cells. *Cancer Cell* **29,** 548–562
37. Martinez-Outschoorn, U. E., Sotgia, F., and Lisanti, M. P. (2012) Power surge: supporting cells "fuel" cancer cell mitochondria. *Cell Metab.* **15,** 4–5
38. Ramanathan, A., Wang, C., and Schreiber, S. L. (2005) Perturbational profiling of a cell-line model of tumorigenesis by using metabolic measurements. *Proc. Natl. Acad. Sci. U.S.A.* **102,** 5992–5997
39. Migneco, G., Whitaker-Menezes, D., Chiavarina, B., Castello-Cros, R., Pavlides, S., Pestell, R. G., Fatatis, A., Flomenberg, N., Tsirigos, A., Howell, A., Martinez-Outschoorn, U. E., Sotgia, F., and Lisanti, M. P. (2010) Glycolytic cancer associated fibroblasts promote breast cancer tumor growth, without a measurable increase in angiogenesis: evidence for stromal-epithelial metabolic coupling. *Cell Cycle* **9,** 2412–2422
40. Lee, P., Vousden, K. H., and Cheung, E. C. (2014) TIGAR, TIGAR, burning bright. *Cancer Metab.* **2,** 1
41. Sun, M., Li, M., Huang, Q., Han, F., Gu, J. H., Xie, J., Han, R., Qin, Z. H., and Zhou, Z. (2015) Ischemia/reperfusion-induced upregulation of TIGAR in brain is mediated by SP1 and modulated by ROS and hormones involved in glucose metabolism. *Neurochem. Int.* **80,** 99–109
42. Quaegebeur, A., Segura, I., Schmieder, R., Verdegem, D., Decimo, I., Bifari, F., Dresselaers, T., Eelen, G., Ghosh, D., Davidson, S. M., Schoors, S., Broekaert, D., Cruys, B., Govaerts, K., De Legher, C., *et al.* (2016) Deletion or Inhibition of the Oxygen Sensor PHD1 Protects against Ischemic Stroke via Reprogramming of Neuronal Metabolism. *Cell Metab.* **23,** 280–291
43. Farmaki, E., Chatzistamou, I., Bourlis, P., Santoukou, E., Trimis, G., Papavassiliou, A. G., and Kiaris, H. (2012) selection of p53-deficient stromal cells in the tumor microenvironment. *Genes Cancer* **3,** 592–598
44. Patocs, A., Zhang, L., Xu, Y., Weber, F., Caldes, T., Mutter, G. L., Platzer, P., and Eng, C. (2007) Breast-cancer stromal cells with TP53 mutations and nodal metastases. *N. Engl. J. Med.* **357,** 2543–2551
45. Semenza, G. L. (2013) HIF-1 mediates metabolic responses to intratumoral hypoxia and oncogenic mutations. *J. Clin. Invest.* **123,** 3664–3671
46. Obach, M., Navarro-Sabaté, A., Caro, J., Kong, X., Duran, J., Gómez, M., Perales, J. C., Ventura, F., Rosa, J. L., and Bartrons, R. (2004) 6-Phosphofructo-2-kinase (pfkfb3) gene promoter contains hypoxia-inducible factor-1 binding sites necessary for transactivation in response to hypoxia. *J. Biol. Chem.* **279,** 53562–53570
47. Chiavarina, B., Martinez-Outschoorn, U. E., Whitaker-Menezes, D., Howell, A., Tanowitz, H. B., Pestell, R. G., Sotgia, F., and Lisanti, M. P. (2012) Metabolic reprogramming and two-compartment tumor metabolism: opposing role(s) of HIF1$\alpha$ and HIF2$\alpha$ in tumor-associated fibroblasts and human breast cancer cells. *Cell Cycle* **11,** 3280–3289
48. Olumi, A. F., Grossfeld, G. D., Hayward, S. W., Carroll, P. R., Tlsty, T. D., and Cunha, G. R. (1999) Carcinoma-associated fibroblasts direct tumor progression of initiated human prostatic epithelium. *Cancer Res.* **59,** 5002–5011
49. Augsten, M., Sjöberg, E., Frings, O., Vorrink, S. U., Frijhoff, J., Olsson, E., Borg, Å., and Östman, A. (2014) Cancer-associated fibroblasts expressing CXCL14 rely upon NOS1-derived nitric oxide signaling for their tumor-supporting properties. *Cancer Res.* **74,** 2999–3010
50. Martinez-Outschoorn, U. E., Goldberg, A., Lin, Z., Ko, Y. H., Flomenberg, N., Wang, C., Pavlides, S., Pestell, R. G., Howell, A., Sotgia, F., and Lisanti, M. P. (2011) Anti-estrogen resistance in breast cancer is induced by the tumor microenvironment and can be overcome by inhibiting mitochondrial function in epithelial cancer cells. *Cancer Biol. Ther.* **12,** 924–938
51. Sanchez-Alvarez, R., Martinez-Outschoorn, U. E., Lamb, R., Hulit, J., Howell, A., Gandara, R., Sartini, M., Rubin, E., Lisanti, M. P., and Sotgia, F. (2013) Mitochondrial dysfunction in breast cancer cells prevents tumor growth: understanding chemoprevention with metformin. *Cell Cycle* **12,** 172–182
52. Hanai, J., Dhanabal, M., Karumanchi, S. A., Albanese, C., Waterman, M., Chan, B., Ramchandran, R., Pestell, R., and Sukhatme, V. P. (2002) Endostatin causes $G_1$ arrest of endothelial cells through inhibition of cyclin D1. *J. Biol. Chem.* **277,** 16464–16469
53. Van Schaftingen, E., Lederer, B., Bartrons, R., and Hers, H. G. (1982) A kinetic study of pyrophosphate: fructose 6-phosphate phosphotransferase from potato tubers. Application to a microassay of fructose 2,6-bisphosphate. *Eur. J. Biochem.* **129,** 191–195
54. Curry, J. M., Tassone, P., Cotzia, P., Sprandio, J., Luginbuhl, A., Cognetti, D. M., Mollaee, M., Domingo-Vidal, M., Pribitkin, E. A., Keane, W. M., Zhan, T., Birbe, R., Tuluc, M., and Martinez-Outschoorn, U. (2016) Multicompartment metabolism in papillary thyroid cancer. *Laryngoscope* **126,** 2410–2418